LAWRENCE
LIVERMORE
NATIONAL
LABORATORY

LLNL-PROC-857831

Experimental and Kinetic modeling of soot formation in counterflow flames of surrogate fuel components: n-dodecane and iso-dodecane

T. Chatterjee, C. Saggese, X. Xue, G. Kukkadapu, W. J. Pitz, S. W. Wagnon, C. J. Sung

December 1, 2023

CI#s 40th International Symposium - Emphasizing Energy Transition
Milan, Italy
July 21, 2024 through July 26, 2024

Disclaimer

Experimental and Kinetic modeling of soot formation in counterflow non-premixed flames of surrogate fuel components: n-dodecane and iso-dodecane

Tanusree Chatterjee[1], Chiara Saggese[1], Xin Xue[2,3], Goutham Kukkadapu[1], William J. Pitz[1], Scott W. Wagnon[1], Chih-Jen Sung[2]*

[1]Materials Science Division, Lawrence Livermore National Laboratory, Livermore, CA 94551, USA

[2]Mechanical Engineering Department, University of Connecticut, Storrs, CT 06269, USA

[3]National Key Laboratory of Science and Technology on Aero-Engine Aero-thermodynamics, Research Institute of Aero-Engine, Beihang University, Beijing, 100191, China

**Corresponding Author Email:chatterjee2@llnl.gov*

Abstract

Normal dodecane (n-C12) and iso-dodecane (i-C12) are often used as components for surrogate mixtures of aviation and diesel fuels. Although studies have been performed to understand the combustion and spray behavior of dodecane isomers, the soot formation from the combustion of n- and i-C12 in non-premixed flames is not well studied. In this work, soot volume fraction (SVF) profiles of n- and i-C12 were measured across a wide range of strain rates and mixture conditions in a counterflow burner facility at the University of Connecticut. Neat and binary mixtures of n- and i-C12 were investigated to study the influence of alkane branching on soot formation. A soot model was developed and validated in this study by extending the detailed kinetic model developed at the Lawrence Livermore National Laboratory (LLNL) for the formation of polycyclic aromatic hydrocarbons (PAHs) to simulate soot formation and growth based on the discrete sectional method. Additional gas phase reactions forming pyrene and ring enlargement reactions were added to the existing PAH model. The LLNL kinetic model was validated with SVF data obtained in this work for n-C12 and i-C12 flames along with data available in literature for ethylene, iso-butene, n-heptane and iso-octane. The soot precursor reactions added in this work were found to play a critical role in simulating the experimentally observed non-linear trend of the peak SVF with increased branched alkanes. Reaction path analysis was conducted to illustrate the fuel structure effects on soot formation pathways in n- and i-C12 mixtures. In view of the satisfactory agreement between modeling results and experimental data, as well as capturing the non-linear variation in peak SVF with the alkane branching for the first time, further investigation within the framework of the soot model is discussed and critical insights are provided into the reaction pathways which require further attention.

Keywords: counterflow non-premixed flame; soot; dodecane isomers; surrogate fuel components; kinetic modeling

*Corresponding author.

LLNL-PROC-857831

Information for Colloquium Chairs and Cochairs, Editors, and Reviewers

1) Novelty and Significance Statement

Normal dodecane (n-C12) and iso-dodecane (i-C12) are commonly used as diesel and jet fuel surrogates. Although soot formation from n-C12 has been studied previously in the literature, soot studies of its highly branched isomer, i-C12, and blends of large n-alkanes and iso-alkanes have been meager. This is the first experimental study to measure soot volume fraction (SVF) in counterflow (CF) flames of n-C12, i-C12, and their blends with an aim to better understand the effects of alkane branching on soot formation and provide new soot measurements for model validation. A new soot model is also proposed and comprehensively validated for the first time across a wide range of CF flames involving commonly used surrogates for real complex fuels. Using the validated model, this study provides critical insight into reactions playing a key role in simulating the experimentally observed non-linearity in peak SVF as alkane branching in the fuel blend increases.

2) Author Contributions

The authors should be identified by their initials and each author's contributions to the manuscript should be indicated by 2-3 words such as, for example, "designed research," "performed research," "analyzed data," "wrote the paper," etc.

- **T.C.** Data curation; formal analysis; investigation; validation; writing – original draft; writing – review & editing.
- **C.S.** Validation; data analysis; supervision; writing – review & editing
- **X.X.** Investigation; formal analysis; data curation; writing – original draft.
- **G.K.** Validation; data analysis; supervision
- **W.J.P.** Writing – review & editing.
- **S.W.W.** Funding acquisition; project administration; supervision; writing – review & editing.
- **C.J.S.** Conceptualization; funding acquisition; project administration; supervision; writing – review & editing.

3) Authors' Preference and Justification for Mode of Presentation at the Symposium

The authors strongly prefer **OPP** presentation at the Symposium, for the following reasons:

- This paper is deemed to have the potential of adding value to the community through a room-audience-level discussion.
- This OPP can focus on outcomes and results without requiring the inclusion of extensive background information.
- We approach the subject that is different to other related work and contextual information is not deemed essential.

1. Introduction

Soot particles resulting from the incomplete combustion of hydrocarbons can lead to significant health hazards as well as global warming [1]. Efforts to mitigate these adverse effects have often taken the form of increasingly stringent emissions standards to reduce soot particulate matter. These stringent standards have made it progressively more challenging to achieve permissible levels of engine out soot using existing devices, fuels, and approaches.

Low-lifecycle carbon and low-sooting fuels such as renewable diesel and synthetic paraffinic kerosene are widely viewed as viable fuels to help mitigate adverse effects stemming from combustion applications. However, one impediment to utilizing combustion with low engine out soot is the inability to design and optimize combustors using predictive simulations of surrogate mixtures for sustainable fuels. Although kinetic models have been developed to simulate soot formation and growth at engine conditions, many studies have focused on ethylene (C_2H_4) as a fuel since it is a significant intermediate formed during combustion [2-5]. Far fewer studies have focused on soot formation during the combustion of heavier fuel components and surrogate mixtures for complex fuels.

For instance, literature studies of reference compounds such as n-heptane (n-C7), iso-octane (i-C8), and toluene provide critical insights into the soot formation of larger linear alkanes, branched alkanes, and aromatics. These reference compounds are also template species for larger, less volatile components found in aviation and diesel fuels. While there are many ways to study the fundamentals of soot formation and growth for fuels, such as using sprays [6] and premixed flames [7], the literature most relevant to this work pertains to non-premixed flames. A very recent example of a single-component fuel includes the study of Zheng et al. [8] and Nobili et al. [9] which investigated soot formation from n-C7 in counterflow (CF) non-premixed flames by performing both experiments and numerical simulations. Also using co-flow non-premixed flames, Kashif et al. [10, 11] and Consalvi et al. [12] studied sooting tendencies of n-C7 and i-C8 binary mixtures. These binary mixture studies agree well with the broader literature which indicates that highly branched alkanes typically produce more soot than linear alkanes. Using CF non-premixed flames, Choi et al. [13] investigated soot formation in binary mixtures of n-C7, i-C8, and toluene. The authors observed a synergistic effect on the formation of polycyclic aromatic hydrocarbons (PAHs) as a function of toluene ratio in the n-C7/toluene and i-C8/toluene flames. Systematic investigations of toluene primary reference mixtures on PAH/soot formation have only been done recently by Park et al. [14] and Kruse et al. [15] by performing both experiments and kinetic modeling studies. For CF flame of n-C7/i-C8, soot volume fraction (SVF) increases non-linearly as i-C8 branching increases. However, for n-C7/toluene and i-C8/toluene flames, Park et al. [14] observed that, although PAHs show a synergistic behavior, SVF increases monotonically as toluene content in the mixture increases.

Measurements of and models for soot formation from surrogate components of diesel and jet fuels, such as n-dodecane and iso-dodecane, are sparser. n-Dodecane (n-C12) is commonly used as a diesel and jet fuel surrogate component to represent the linear paraffins in complex fuels. In addition to being a surrogate component for complex fuels, iso-dodecane (i-C12; 2,2,4,6,6-pentamethylheptane) is also a primary reference compound for cetane measurements. Skeen and Yasutomi [6] studied soot growth for n-C12 in a high-pressure constant-volume spray chamber and observed that under high-pressure pyrolyzing conditions, the maximum rate of soot formation increases linearly with ambient temperature. Furthermore, a critical temperature of 1550 K was observed above which the total soot mass did not increase with ambient temperature. Using a coflow non-premixed burner, Mitra et al. [16] studied the growth of PAHs and young soot from n-C12. The authors observed a rapid increase in PAHs when young soot transitions to a mature one. Wang et al. [17] proposed a reduced PAH mechanism for n-C12. The proposed PAH model was validated with ignition delays and species concentration profiles from shock tubes and jet stirred reactors (JSR). To the authors' knowledge, soot formation studies of n-C12 and i-C12 have not been previously performed in a CF non-premixed flame.

In this study, new soot volume fraction measurements from soot formation in non-premixed flames of neat n-C12 and i-C12 were acquired using the University of Connecticut CF burner facility. Binary mixtures of n-C12 and i-C12 were also studied to better understand how large linear and branched alkanes directly relevant to sustainable aviation fuels influence soot formation in non-premixed CF flames. This is the first study to present SVF data from CF soot formation flames of n-C12, i-C12, and their binary mixtures. In addition, the LLNL model for PAHs [18] was updated and paired with a new soot model based on the discrete sectional method [19,20] proposed in this work.

The developed soot model was then validated with SVF data obtained in this work for n-/i-C12 flames. Additional validations considered literature measurements of SVF and soot precursors. Validation efforts in this work invoked a wide range of CF soot formation flames, including common surrogate fuel components, such as n-C7 and i-C8, and their blends. The use of n-C7 and i-C8 as additional validation cases establishes support for the current implementation of soot formation and growth rate

rules since n-C7 and i-C8 have similar molecular features and intermediate species to the heavier n-C12 and i-C12 components. In addition, the reaction path analysis provides a basis for the discussion of fuel molecular structure effects on soot formation pathways in CF non-premixed flames of n-C12 and i-C12.

2. Experimental specification

Two aerodynamically-converging opposing nozzles of 10 mm exit diameter with a separation distance of 11 mm were placed opposed to each other. Both fuel and oxidizer streams were diluted with nitrogen before flowing into the bottom and top nozzles, respectively. A shroud of nitrogen gas was used to isolate the resulting flame from the ambient air. The flow system and the CF burner were maintained at a temperature of 473±2 K to prevent condensation of pre-vaporized fuel. The laser-induced incandescence (LII) technique was combined with the light extinction (LE) method to measure the soot volume fraction profiles in CF sooting flames. In the LE measurements, a continuous He-Ne laser beam with a wavelength of 632.8 nm was used and a refractive index (m) of 1.57-0.56i was adopted for the current study, which is widely used in literature, as discussed in [21]. For the current experiments, the standard deviation of the LE measurements is less than 5% based on three consecutive runs, while the standard deviation of the LII measurements is less than 18% based on 40 LII images. To study how the alkane branching effect influences soot formation in non-premixed CF flames, several binary mixtures of i-C12 and n-C12 at liquid volume ratios of 25/75, 50/50, 75/25, 90/10, and 95/5 were considered. The mixture compositions and corresponding notations are summarized in Table 1. Further details of the experimental specifications and test conditions are provided in the SM (Discussion 1).

Table 1: Test conditions for i-C12 (2,2,4,6,6-pentamethyheptane) and n- C12 blends studied.

X_F	X_{O_2}	Z_{st}	K (s^{-1})
0.138	0.50	0.237	200–500
0.117	0.45	0.238	
0.100	0.40	0.236	200

X_F: fuel mole fraction in the fuel stream; X_{O2}: oxygen mole fraction in the oxidizer stream; Z_{st}: stoichiometric mixture fraction<0.5 (soot formation flame); K: global strain rate

3. Kinetic model development and numerical simulation

The current work extends the detailed kinetic model developed at LLNL for the formation of PAHs [18] to soot formation and growth. The developed soot model is based on the discrete sectional method. Following a similar methodology as Saggese et al. [19], heavy PAHs and soot particles are discretized into 20 sections of lumped species, i.e., BIN*n* with *n*=1-20, with carbon atoms ranging from 20 in BIN1 to 10^7 in BIN20. For all BIN*n*, only one hydrogenation level is considered which greatly reduces the number of species and reactions in the model. The primary soot reaction classes and their related references for the kinetic parameters used in this study are summarized in Table 2.

Table 2: Main soot reaction classes.

Soot reaction classes	References
1. HACA H abstraction from BIN(M) C_2H_2 addition to BIN(R)	C_6H_5+H/CH_3 from [22] C_6H_5+OH from [23] C_6H_5+C_2H_2 from [24]
2. Soot inception PAH(R/M)+PAH(R/M) BIN_i(i<5) + BIN_j(j<5)	BIN+BIN from [20] C_6H_5+C_6H_5 from [27] C_6H_5+C_6H_6 from [28]
3. Surface growth RSR + BIN (R/M) PAH (R) + BIN (R/M) BIN_i(i<5) + BIN_j(j>5)	BIN+BIN from [20] C_3H_3+C_6H_5 from [25] C_3H_3+C_6H_6 from [26] C_6H_5+C_6H_5 from [27] C_6H_5+C_6H_6 from [28]
4. Particle coalescence and aggregation BIN_i(i>5) + BIN_j(j>5)	BIN+BIN from [20]

R=radical; M=molecule; RSR=Resonance stabilized radicals: C_3H_3, i-C_4H_5, i-C_4H_3, C_5H_5, C_3H_5-A, C_7H_7, C_9H_7; PAH=polycyclic aromatic hydrocarbons: A1-A4.

It is well known that the H-atom abstraction (H+BIN*n*), acetylene addition to BIN radicals (C_2H_2+BIN*n*J) (i.e., HACA) reaction class plays a critical role in soot inception and growth [19,20]. In the LLNL model, rate parameters for HACA are based on theoretical studies [22-24] using benzene (C_6H_6) and phenyl radicals (C_6H_5) as reference aromatics. To consider the effect of the size of the soot particle on rate parameters of C_2H_2 addition to BIN radicals, the A-factors have been scaled according to the size of the particle [22]. In addition to C_2H_2, odd carbon numbered resonance stabilized radicals (RSRs) are also known to play critical role in soot formation and growth [14]. Reactions involving propargyl (C_3H_3) radicals were found to be highly sensitive to SVF in the sensitivity analysis performed in this study (Fig. SM1). In the proposed model, rate constants for RSR+BIN*n*J reactions are based on a recent theoretical study by Mebel and coworkers [25] involving C_6H_5 and C_3H_3. To consider the change in collision frequency with the increasing diameter of soot particles and aggregates, the A-factors have been

scaled for surface growth reactions according to the methodology proposed by Pejpichestakul et al. [4]. Reactions of PAH addition to BIN radicals also contribute significantly to soot inception and growth [19,20]. In this study, rate constants for surface growth reactions involving light PAH radicals up to pyrene (A4) are based on theoretical studies involving self-reaction of phenyl radicals (i.e., $C_6H_5+C_6H_5$) [27]. Rate constants for surface growth involving heavy PAHs, i.e., BIN1-4 and soot particles (BIN5-12) /aggregates (BIN13-20) are based on Ref. 20. Rate constants for soot reaction class 4 i.e., particle coalescence and aggregation which involves interactions only between soot particles and soot aggregates are also based on Ref. 20. Interactions only between heavy PAHs (BIN1-4) result in the first soot particle i.e., BIN5 called soot inception (soot reaction class 2). Rate constants for interactions between heavy PAHs (BIN1-4) are also based on Ref. 20. Soot inception reaction class also includes interactions between light PAHs leading to form BIN1 and/or BIN2. Rate constants for interactions between light PAHs are based on analogy to reactions: $C_6H_5+C_6H_5$ from [27] and $C_6H_5+C_6H_6$ from [28].

The existing PAH model from LLNL [18] was updated by adding new lumped reactions involving C_9H_7 and C_7H_7 radicals to form pyrene ($C_{16}H_{10}$, A4) based on the study by Park et al. [14]. New ring enlargement reactions involving phenanthrene (A3) and pyrene (A4) radicals were added to form BIN1. The newly added reactions play a critical and sensitive role in CF of i-C12 and i-C8 flames studied in this work.

Simulations of SVF were performed using the unsteady counterflow non-premixed flame code developed at LLNL [29], with constant Lewis number approximations for each species. Applying a constant Lewis number approximation reduces the wall time of simulations by as much as a factor of 10 compared to using mixture-averaged transport approach for CF flames calculations involving large surrogate components, such as n-C12 and i-C12. Effects of thermophoresis and particle diffusivity coefficients computed through a Stokes–Cunningham correlation on simulations of SVF are provided in Figs.SM2-3. Thermophoresis typically shifts the SVF peak towards the fuel side, while utilizing Stokes–Cunningham diffusivity coefficients changes the shape of the SVF profile as well as increasing peak SVF. Reaction path analysis was performed with CHEMKIN Pro [30] to facilitate discussion of fuel molecular structure effects on SVF.

4. Results and Discussion

4.1. Experimental results and model validation studies

A selection of the experimental results along with the corresponding simulations of SVF from the CF flame of neat n-C12, i-C12, and their binary mixtures are shown in panels a) and b) of Fig. 1. Additional SVF measurements and validations from this work are provided in the SM (Fig. SM4). As expected, it can be seen that the peak SVF along the centerline and the overall soot loading increase with higher concentrations of i-C12 in the fuel blend. Furthermore, it can be observed that as K increases, peak SVF decreases as expected due to the reduction in characteristic residence time within the flame. These observations are consistent with literature studies comparing soot formation for linear and branched alkanes [14,15]. A more thorough discussion of fuel molecular structure effects on SVF is provided in Section 4.2. It can also be observed from Fig. 1(a) that peak SVF values increase non-linearly as a function of i-C12 content in the fuel blend. In particular, when the i-C12 concentration is greater than 90% in the blend, peak SVF exhibits a stronger non-linear increase. This non-linearity in peak SVF data has already been reported by Park et al. [14] for CF non-premixed flames of i-C8 and n-C7 blends, as shown in Fig. 1c. Simulations using the LLNL model can capture the non-linear increase of peak SVF with iC12 content reasonably well across the wide range of strain rates considered in this study. The LLNL model also captures the non-linear trend in peak SVF for n-C7/i-C8 blends reported by Park et al. [14], as seen in Fig 1c. The simulation is also able to qualitatively capture the strain rate dependence with peak SVF.

Figure 1b compares the spatially resolved SVF profiles along the centerline of flame. The x axis is the distance from the fuel nozzle normalized to the location of the peak SVF in i-C12. The peak values of each SVF curve were observed to occur at approximately 3.96 mm from the fuel nozzle, suggesting that the location of peak LII signal is independent of i-C12/n-C12 blending ratio when keeping Z_{st} constant. Furthermore, the overall thickness of the SVF profiles appears similar for all fuel blends, as K is kept constant. It can be observed from Fig. 1b that the simulated SVF profile matches well with the data.

Regarding quantitative agreement, the simulations tend to overpredict SVF of C12 mixtures by a factor of 5 for all conditions studied in this work. In addition to the validations against SVF data obtained in this study for n-/i-C12, the LLNL model was also validated with literature data for CF flames of n-C7 and i-C8, which are common surrogate fuel components and have similar molecular structures to n-C12 and i-C12, respectively. From validation studies shown in Figs. 1c and SM5-6, it can be observed that simulations predict peak SVF for CF flames of n-C7 and i-C8 within a factor of 3. The LLNL model was also validated with the SVF data available in literature for C_2H_4 counterflow flames, which have been commonly used in the literature to

validate soot models. These validations for C_2H_4 mixtures are provided in the SM (Fig. SM7) and the LLNL model underpredicts the SVF data for C_2H_4 flames by as much as a factor of 4.

While evaluating the LLNL model for quantitative agreement of SVF, it is notable that there exists a systematic uncertainty in SVF measurements using the LE technique. This uncertainty is of a factor 3 stemming from the assignment of the refractive index value used to convert raw signals to SVF while calibrating the LII signals against LE measurements [3,15,21,31,32]. It has also been discussed in the literature that the choice of diagnostic wavelength potentially introduces additional systematic bias into SVF measurements [31]. As addressed in Section 3, decisions regarding the exclusion of thermophoretic effects and estimation of particle diffusivity coefficients can also influence the simulated SVF of CF flames. Therefore, in this work quantitative agreement of simulations with SVF measurements within a factor of 5 was considered reasonably accurate.

To the best of authors' knowledge, this is the first study to capture both the experimentally observed non-linear trend and the absolute value of peak SVF for n-alkane and highly branched alkane flames reasonably well. For example, although Park et al. [14] in their study used the soot model from Wang et al. [33] to simulate the non-linear trend in peak SVF for n-C7/i-C8 mixtures, their model comparisons only showed normalized SVF data. Furthermore, although the latest soot model published by Nobili et al. [20] can capture peak SVF for n-C7/i-C8 mixtures in CF flames within a factor of 3, it is not able to capture the non-linear trend in peak SVF reported by Park et al. [14]. Comparisons illustrating this point are provided in the SM (Fig. SM8).

In addition to SVF validations, the LLNL model was validated with measurements of smaller intermediate species including PAHs under similar flame conditions. Validations of the LLNL model for species from CF flames of n-C7, i-C8, C_2H_4, and iso-butene (i-C4) are provided in the SM (Figs. SM9-13). iso-Butene was included since it is one of the primary intermediates in both i-C8 and i-C12 flames. To the best of our knowledge, there is no speciation data available for CF flames of n-C12 and i-C12 which could further validate modeled pathways to soot formation. The LLNL model can simulate the mole fraction of small gas phase species reasonably well for all CF flames studied in this work (within a factor of 2), while overpredicting the mole fraction of C_6H_6. However, other aromatics such as toluene, styrene, naphthalene, phenanthrene etc. are captured reasonably well (within a factor of 3) for all flames. Taken together, these comprehensive validations demonstrate an effort to evaluate and improve the LLNL model using a wide range of CF flame

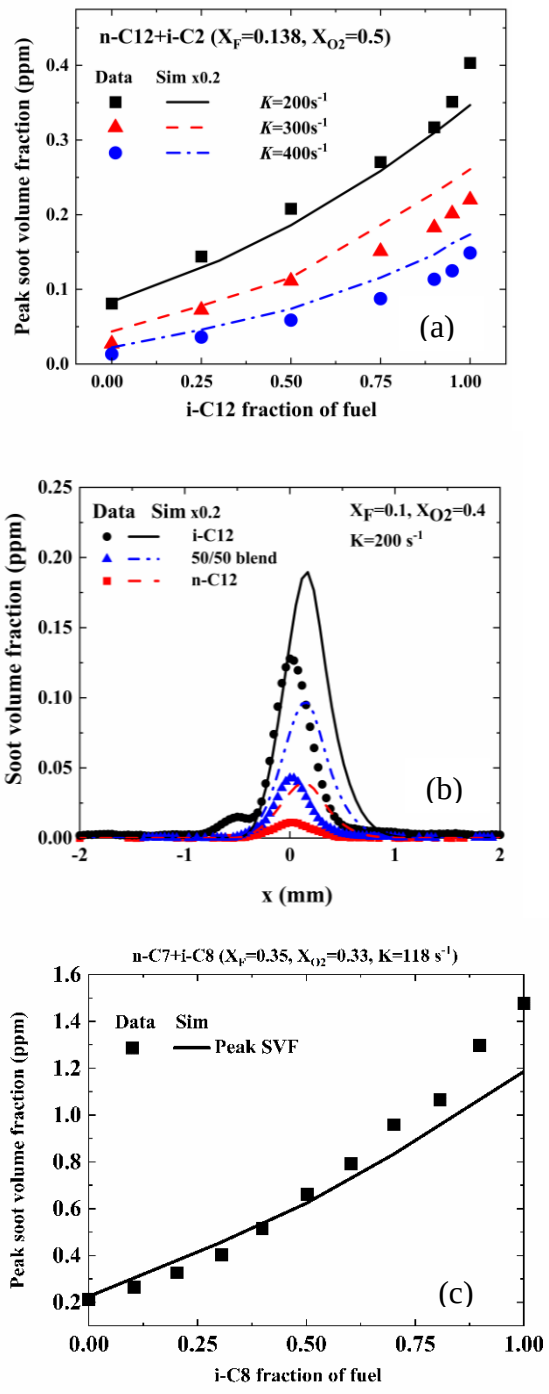

Figure 1. Comparison of SVF measurements and simulations for: a) i-C12 and n-C12 flames vs i-C12 liquid volume fraction in the fuel blend; b) i-C12 and n-C12 flames along the centerline; c) i-C8 and n-C7 flames vs i-C8 fraction in the fuel blend.

conditions and mixtures, including common surrogate components sharing structural similarities.

4.2 Chemical kinetic analysis and discussion of alkane branching influence on SVF

Rate of production analysis (ROPA) using CHEMKIN Pro [30] was performed to identify the differences in reaction pathways for PAH formation in CF flames of n-/i-C12 mixtures. Fig. 2 shows the simplified ROPA for benzene (C_6H_6, A1), naphthalene ($C_{10}H_8$, A2), phenanthrene ($C_{14}H_{10}$, A3) and pyrene ($C_{16}H_{10}$, A4). A detailed ROPA for A1-A4 is provided in the SM (Figs. SM14-15). To identify possible reasons for the non-linear increase in SVF as i-C12 content increases, the evolution of critical intermediates (C1-C9) along with PAH/soot precursors were investigated. Additional simulations were run to identify reactions which play a critical role in simulating the experimentally observed non-linear trend in SVF.

The ROPA shows that primary pathways for A1-A4 formation remain similar for both n-C12 and i-C12. Benzene (A1) is primarily formed via ring expansion reactions preceded by addition of methyl radicals to cyclopentadienyl radical in both flames. Once formed, benzene undergoes H-atom abstraction to form phenyl radicals which react with allyl radical (C_3H_5-A) to form indenyl (C_9H_8) which undergoes ring enlargement reactions via H-atom abstraction and addition of methyl radicals to form naphthalene ($C_{10}H_8$, A2). Phenyl radicals also react with other intermediate species (CH_3, C_2H_4, C_2H_2, C_4H_6) to form naphthalene (A2). A2 is also formed through another major pathway involving propargyl (C_3H_3) and fulvenallenyl (C_7H_5) radicals which is primarily formed via reactions involving only C_2H_2 and C_3H_3. From Fig. SM16(a) it can be observed that while the mole fraction of C_2H_2 reduces as alkane branching increases, the mole fraction of C_3H_3 increases. Similar conclusion was also made by Park et al. [14] in their study on CF flames of n-C7 and i-C8. The increased mole fraction of C_3H_3 with alkane branching leads to a higher percentage of A2 formed via fulvenallenyl and propargyl pathway in i-C12 flame. Similar to A2, phenanthrene (A3) is also formed via similar ring enlargement and ring closure reactions involving benzene, naphthalene and intermediate species such as CH_3, C_2H_2, C_3H_3, C_5H_5. A3 thus formed undergoes H-atom abstraction and subsequent C_2H_2 addition (HACA) to form pyrene (A4). Pyrene is also formed via newly added pathways involving two RSRs, indenyl (C_9H_7) and benzyl (C_7H_7) radicals [14] (R1: $C_9H_7+C_9H_7=>A4+C_2H_2+H_2$; R2: $C_9H_7+C_7H_7=>A4+2H_2$). As i-C12 content increases, the percentage of A4 formed via R1 and R2 increases. Among PAHs, only A4 shows significant non-linearity as branching increases (Fig. SM16(b)). Park et al. [14] also observed in their experiments that larger PAHs such as pyrene exhibit a non-linear increase with i-C8 blending ratio. From Fig. SM16(a), it is observed that mole fractions of indenyl and benzyl radicals increase non-linearly with i-C12 blending ratio which possibly explains the non-linear increase in mole fraction of A4. Additional simulations were performed by removing R1 and R2 to further confirm the role of C_7H_7 and C_9H_7 in A4 formation as alkane branching increases (Figs. SM17-18). It has been observed from these simulations that without R1 and R2 in the LLNL model, the model is no longer able to simulate the non-linear evolution of pyrene as alkane branching increases. Furthermore, it has been observed that without R1 and R2 in the model, the rate of increase in A4 with alkane branching reduces significantly and is lower than smaller PAHs which would contradict experimental observations made by Park et al. [14]. In addition, from Fig. 3 it can be observed that without R1 and R2 in the LLNL model, simulations fail to capture the non-linearity observed during experiments in the evolution of peak SVF with alkane branching. Newly added ring enlargement reactions involving A3 and A4 were also found to be important in predicting the non-linearity accurately. From Fig. 3 it can be observed that removing all the newly added gas phase PAH reactions from the model leads to significant reduction in simulated peak SVF for i-C12 flame and changes the peak SVF profile to be almost linear with alkane branching. It is to be noted that there is no significant effect of newly added gas phase PAH reactions on simulated SVF for n-C12 flame. Similar observations were also made for CF flame of n-C7, i-C8 and their blends. Given the importance of the additional soot precursor reactions in capturing the non-linear trends in peak SVF, further experimental and theoretical studies of these reactions and their related potential energy surfaces are necessary.

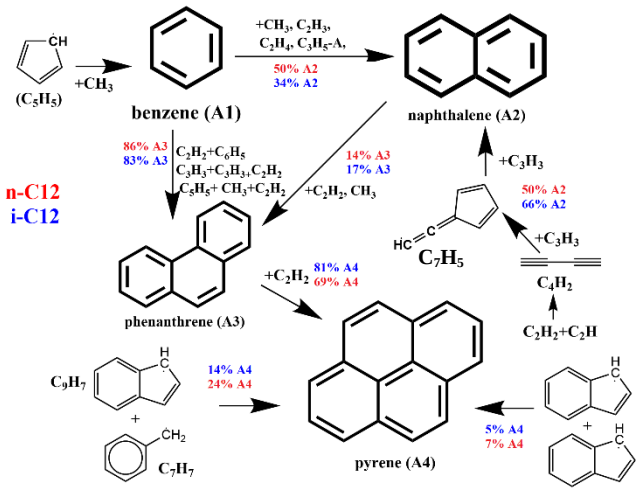

Figure 2. Reaction path analysis for A1-A4 in CF flames of neat n-C12 and i-C12 at 1300 K (X_F=0.138, X_{O2}=0.5, K=200 s^{-1}).

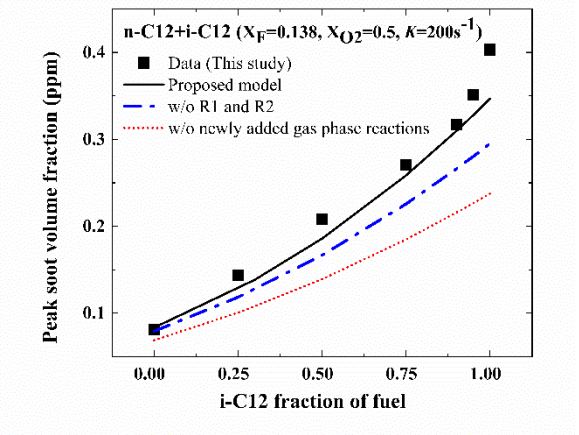

Figure 3. Simulations of peak SVF with and without additional soot precursor reactions, see main text for details.

5. Conclusion

Soot formation from the combustion of n-C12 and i-C12 was studied in counterflow non-premixed flames. This work is the first experimental study to measure SVF in CF flames of n-C12 and i-C12 which are commonly used as diesel and aviation surrogate fuel components. Soot volume fractions were measured for several global strain rates and fuel loadings for a fixed stoichiometric mixture fraction. The role of linear and branched fuel structures on the formation of soot was investigated using several binary mixtures of n-C12 and i-C12. As expected, the measurements show that peak SVF for n-C12, i-C12, and their binary mixtures decrease with increasing global strain rate. This work demonstrates that peak SVF increases non-linearly with i-C12 content, agreeing with the observations of Park et al. [14] for n-C7 and i-C8 which share similar structural features.

To simulate these measurements, the PAH model previously developed at LLNL was extended to model soot formation. New reactions involving indenyl, benzyl, propargyl, and methyl radicals forming pyrene and heavier PAHs were added to the PAH submodel. These reactions were observed to play a critical role in CF flames of highly branched alkanes such as i-C12 and i-C8. The LLNL soot model coupled with the updated PAH model was validated with the data obtained in this work for CF flames of n- and i-C12.

Additional experimental data available from literature was used to comprehensively validate the model for CF flames of n-C7, i-C8, C_2H_4, and iso-butene mixtures. Comparisons show that the LLNL model can capture the data qualitatively well across a wide range of strain rates and mixture conditions. Regarding quantitative agreement, the simulated SVF is typically within a factor of 5. Given the systematic uncertainty of a factor of 3 associated with SVF measurements, simulations of SVF within a factor of 5 can be considered reasonably accurate. More importantly, the current LLNL model with the newly added soot precursor reactions is able to capture, for the first time, the non-linear variation in peak SVF with the alkane branching. Furthermore, using the validated model developed in this work, this study provides important insights into the reaction pathways which require further investigation to bridge quantitative gaps that remain in accurately predicting soot formation for surrogate fuel components of aviation and diesel fuels.

Acknowledgements

This work was performed under the auspices of the U.S. Department of Energy by LLNL under Contract DE-AC52-07NA27344 as part of the Decarbonization of Off-Road, Rail, Marine, and Aviation program sponsored by the DOE Office of Energy Efficiency and Renewable Energy Vehicles Technologies Office with managers Gurpreet Singh and Kevin Stork.

Supplementary materials

Experimental data, kinetic model with thermodynamic and transport files, additional model validation studies and discussion.

References

[1] T. C. Bond et al., Bounding the role of black carbon in the climate system: A scientific assessment, J. Geophys. Res. Atmos 18 (2013) 5380–5552.

[2] Y. Wang, S.H. Chung, Soot formation in laminar counterflow flames, Prog. Energy Combust. Sci. 74 (2019) 152–238.

[3] K. Gleason, F. Carbone, A. Gomez, Effect of temperature on soot inception in highly controlled counterflow ethylene diffusion flames, Combust. Flame 192 (2018) 283–294.

[4] W. Pejpichestakul, A. Frassoldati, A. Parente, T. Faravelli, Soot Modeling of Ethylene Counterflow Diffusion Flames, Combust. Sci. Technol. 191 (2019) 1473–1483.

[5] X. Xue, P. Singh, C.J. Sung, Soot formation in counterflow non-premixed ethylene flames at elevated pressures, Combust. Flame 195 (2018) 253–266.

[6] S.A. Skeen, K. Yasutomi, Measuring the soot onset temperature in high-pressure n-dodecane spray pyrolysis, Combust. Flame 188 (2018) 4 83–4 87.

[7] A. D'Anna, A. Ciajolo, M. Alfe, B. Apicella, A. Tregrossi, Effect of fuel/air ratio and aromaticity on the molecular weight distribution of soot in premixed n-heptane flames, Proc. Combust. Inst 32 (2009) 803–810.

[8] D. Zheng, A. Nobili, A. Cuoci, M. Pelucchi, X. Hui, T. Faravelli, Soot formation from n-heptane counterflow diffusion flames: Two-dimensional and oxygen effects, Combust. Flame 258 (1) (2023) 112441.
[9] A. Nobili, D. Zheng, M. Pelucchi, A. Cuoci, A. Frassoldati, X. Hui, et al., Oxygen effects on soot formation in H_2/n-heptane counterflow flames, Combust. Flame 253 (2023) 112821.
[10] M. Kashif, P. Guibert, J. Bonnety, G. Legros, Sooting tendencies of primary reference fuels in atmospheric laminar diffusion flames burning into vitiated air, Combust. Flame 161 (2014) 1575–1586.
[11] M. Kashif, J. Bonnety, A. Matynia, P. Da Costa, G. Legros, Sooting propensities of some gasoline surrogate fuels: Combined effects of fuel blending and air vitiation, Combust. Flame 162 (2015) 1840–1847.
[12] J.L. Consalvi, F. Liu, J. Contreras, M. Kashif, G. Legros, S. Shuai, J. Wang, Numerical study of soot formation in laminar coflow diffusion flames of methane doped with primary reference fuels, Combust. Flame 162 (2015) 1153–1163.
[13] B.C. Choi, S.K. Choi, S.H. Chung, Soot formation characteristics of gasoline surrogate fuels in counterflow diffusion flames, Proc. Combust. Inst 33 (2011) 609–616.
[14] S. Park, Y. Wang, S.H. Chung, S.M. Sarathy, Compositional effects on PAH and soot formation in counterflow diffusion flames of gasoline surrogate fuels, Combust. Flame 178 (2017) 46–60.
[15] S. Kruse, A. Wick, P. Medwell, A. Attili, J. Beeckmann, H. Pitsch, Experimental and numerical study of soot formation in counterflow diffusion flames of gasoline surrogate components, Combust. Flame 210 (2019) 159–171.
[16] T. Mitra, T. Zhang, A.D. Sediako, M.J. Thomson, Understanding the formation and growth of polycyclic aromatic hydrocarbons (PAH) and young soot from n-dodecane in a sooting laminar coflow diffusion flame, Combust. Flame 202 (2019) 33–42.
[17] H. Wang, Y. Ra, M. Jia, R.D. Reitz, Development of a reduced n-dodecane-PAH mechanism and its application for n-dodecane soot predictions, Fuel 136 (2014) 25–36.
[18] G. Kukkadapu, S.W. Wagnon, W.J. Pitz, N. Hansen, Identification of the molecular-weight growth reaction network in counterflow flames of the C3H4 isomers allene and propyne. Proc Combust Inst., 38 (2021) 1477-1485.
[19] C. Saggese, S. Ferrario, J. Camacho, A. Cuoci, A. Frassoldati, E. Ranzi, H. Wang, Tiziano Faravelli, Kinetic modeling of particle size distribution of soot in a premixed burner-stabilized stagnation ethylene flame, Combust. Flame 162 (2015) 3356–3369.
[20] A. Nobili, A. Cuoci, W. Pejpichestakul, M. Pelucchi, C. Cavallotti, T. Faravelli, Modeling soot particles as stable radicals: a chemical kinetic study on formation and oxidation. Part I. Soot formation in ethylene laminar premixed and counterflow diffusion flames, Combust. Flame 23 (2022) 112073.
[21] P. Singh, X. Hui, C.J. Sung, Soot formation in non-premixed counterflow flames of butane and butanol isomers, Combust. Flame 164 (2016) 167-182.
[22] A. S. Semenikhin, A. S. Savchenkova, I. V. Chechet, S. G. Matveev, Z. Liu, M. Frenklach, A. M. Mebel. Rate constants for H abstraction from benzo(a)pyrene and chrysene: a theoretical study. Phys. Chem. Chem. Phys., 19 (2017) 25401-25413.
[23] T. Seta, M. Nakajima, A. Miyoshi, High-Temperature Reactions of OH Radicals with Benzene and Toluene, J. Phys. Chem. A 110 (2006) 5081-5090.
[24] A. M. Mebel, Y. Georgievskii, A. W. Jasper, S. J. Klippenstein. Temperature- and pressure-dependent rate coefficients for the HACA pathways from benzene to naphthalene. Proceedings of the Combustion Institute 36 (2017) 919–926.
[25] A. N. Morozov, A. M. Mebel, Theoretical study of the reaction mechanism and kinetics of the phenyl + propargyl association, Phys.Chem.Chem.Phys., 22 (2020) 6868.
[26] V. V. Kislov, A. M. Mebel, Ab Initio G3-type/Statistical Theory Study of the Formation of Indene in Combustion Flames. I. Pathways Involving Benzene and Phenyl Radical, J. Phys. Chem. A 111 (2007) 111, 3922-3931.
[27] R. S. Tranter, S. J. Klippenstein, L. B. Harding, B. R. Giri, X. Yang, J. H. Kiefer. Experimental and Theoretical Investigation of the Self-Reaction of Phenyl Radicals. J. Phys. Chem. A 114 (2010) 8240–8261.
[28] J. Park, S. Burova, A. S. Rodgers, M. C. Lin. Experimental and Theoretical Studies of the C6H5 + C_6H_6 Reaction. J. Phys. Chem. A 103 (1999) 9036-9041.
[29] S. Lapointe, R. A. Whitesides, and M. J. McNenly, Sparse, iterative simulation methods for one-dimensional laminar flames, Combust. Flame 204 (2019) 23-32
[30] CHEMKIN-PRO, Reaction Design, Inc San Diego, CA, 2011.
[31] E. Quadarella, J. Guo, H.G. Im, A consistent soot nucleation model for improved prediction of strain rate sensitivity in ethylene/air counterflow flames, Aerosol Sci Technol. 56 (2022) 7 636–654.
[32] K. Wan, X. Shi, H. Wang, Quantum confinement and size resolved modeling of electronic and optical properties of small soot particles, Proc Combust Inst. 38 (2021) 1517–1524.
[33] Y. Wang, A. Raj, S.H. Chung, Soot modeling of counterflow diffusion flames of ethylene-based binary mixture fuels, Combust. Flame 162 (2015) 586–596.